8 Coexistence of Attractors and Homoclinic Loops in a Kaldor-Like Business Cycle Model

Anna Agliari and Roberto Dieci

8.1 Introduction

Coexistence of attractors is often a characteristic feature of economic models represented by nonlinear dynamic systems [see, among others, Agliari *et al.* (2002), Bischi & Kopel (2001), Dieci *et al.* (2001), Agliari *et al.* (2000)]. Generally speaking, when multiple attractors coexist in the phase-space for a particular choice of the parameters of the model, a crucial question is about the role played by the initial conditions in determining the asymptotic behavior of the system. Moreover, in order to perform a proper bifurcation analysis with respect to some specific parameters it is necessary to take into account that parameter variations determine in general both qualitative changes (including appearance/disappearance) of the attractors, and structural changes of the basins of attraction of the coexisting attractors. The latter point has been less emphasized in the economic literature. In general, typical features of such qualitative changes of the basins are the following: (a) they are due to *global* bifurcations (not associated with the eigenvalues of the linearized system around a particular steady state) and (b) they may bring about a kind of "complexity" which is different from the one usually reported in the literature (associated with "strange attractors", and "sensitivity to initial conditions"): Namely, simple attractors (steady states, cycles of low period, attracting closed curves) may have basins with complex structures.

In recent years, several studies have pointed out particular mechanisms of basin bifurcations, which are associated with contacts between basin boundaries and "critical sets", in the case of dynamical systems represented by the iteration of *noninvertible maps* [Mira *et al.* (1996), Agliari *et al.* (2002), Agliari (2001)]. Other possible mechanisms, which may occur in the case of *invertible maps* as well, are associated with homoclinic tangencies of the

stable and unstable manifolds of saddles. The present Chapter illustrates the latter type of phenomena, in situations of coexisting attractors that arise from a particular version of Kaldor's business cycle model in discrete time, described by a nonlinear two-dimensional dynamical system.

The particular Kaldor-like model at hand, where consumption is modelled as an S-shaped function of income, and investment is a linear increasing function of output (and a linear decreasing function of capital), has been developed in Herrmann (1985), and studied also in Lorenz (1992, 1993), Dohtani *et al.* (1996), mainly in order to prove the emergence of chaotic dynamics in Kaldor-like models under extreme values of the output adjustment parameter. However, the particular parameter constellation which is assumed within the present Chapter (under which multiple equilibria exist) has been excluded from the analysis carried out in earlier work, though it corresponds to economically meaningful situations. We will show that for this choice of parameters, business fluctuations along a stable closed curve (which typically arise in Kaldor model), coexist with alternative dynamic outcomes (stable steady states, or stable periodic orbits of low period), which the system may reach in the long-run depending on the initial state. Furthermore, we will explain the bifurcation mechanisms which determine such situations of coexistence, the appearance or disappearance of attractors and the qualitative changes of the basins of attraction. The global dynamic phenomena which are detected in this Chapter are described in Chapter 1 and have also been detected in a different version of the Kaldor model in discrete-time [see Bischi *et al.* (2001) and Agliari *et al.* (2005b)], where investment is an increasing S-shaped function of output (and depends negatively on capital stock) and savings depend linearly on income. Therefore such dynamic phenomena seem to be very persistent ones, and their occurrence seems to be ultimately related to the following basic assumptions: (i) investment or consumption have sigmoid shaped graphs, in a way that the marginal propensity to invest is larger (smaller) than the marginal propensity to save for normal (extreme) levels of income, and (ii) the investment schedule shifts downwards (upwards) as output increases (decreases) as a result of a negative dependence on accumulated stock of capital. Both these assumptions are essential qualitative features of Kaldor's original model. On the other hand, very similar dynamic phenomena have been detected also in Agliari *et al.* (2005a), where a two-dimensional map with a "minimal" structure qualitatively similar to that in Agliari *et al.* (2005b), and to the one being studied here, has been analyzed in details. Further examples are shown in this book, Chapters 9 and 11.

The Chapter is organized as follows. In Section 8.2 we present the business cycle model, perform useful changes of coordinates, and reduce it to a two-dimensional map. Section 8.3 presents some general properties of the map, namely the symmetry, the steady states and local asymptotic stability conditions, and the conditions for invertibility. Section 8.4 focuses on particular global bifurcations, involving qualitative changes of the basins of attraction, occurring in a particular regime of parameters where three equilibria exist, and relates these phenomena to the behavior of the stable and unstable manifolds of saddles.

8.2 The Model

Let us consider the following discrete-time version of the Kaldor (1940) nonlinear model of the business cycle

$$\begin{cases} Y_{t+1} = Y_t + \alpha\left(I_t - (Y_t - C_t)\right) \\ K_{t+1} = I_t + (1-\delta)\, K_t \end{cases} \tag{1}$$

where the dynamic variables Y_t and K_t represent the income (or output) level and the capital stock in period t, respectively, and both the investment I_t and the consumption C_t (or equivalently the savings $S_t = Y_t - C_t$) are assumed to depend in general on Y_t and K_t.

The first equation in (1) views the output level as reacting over time to the excess demand or, put differently, to the difference between ex-ante investment (I_t) and saving ($S_t = Y_t - C_t$). The *speed of adjustment* is measured by the parameter α ($\alpha > 0$), where a value of α smaller than 1 means a prudent reaction by firms, while a value of α greater than 1 denotes rash reactions and coordination failure.

The second equation in (1) models the capital stock as being increased by realized investment (here assumed to coincide with ex-ante investment) $I_t = I_t(Y_t, K_t)$, and decreased by depreciation δK_t, where δ ($0 < \delta < 1$) represents the *capital stock depreciation rate*.

The discrete dynamical equations (1) (or, alternatively, their continuous-time counterparts) provide the common structure of several versions of the Kaldor model, which have been proposed in the literature up to now [see Dana & Malgrange (1984), Herrmann (1985), Grasman & Wentzel (1994), Bischi *et al.* (2001), among others]. Such models are able to produce both periodic or quasi-periodic trajectories and further dynamic scenarios, ranging from chaotic fluctuations to coexistence of different attractors, once the investment and the savings function I_t and S_t are specified in a way consistent with Kaldor's original qualitative assumptions, namely (a): $\partial I/\partial Y >$

$\partial S/\partial Y$ (i.e. propensity to invest higher than the propensity to save) for "normal" levels of income, but $\partial I/\partial Y < \partial S/\partial Y$ for extreme income levels, below and above the "normal" range; (b) $\partial I/\partial K < 0$, i.e. a negative relationship between investment and capital stock, or $\partial S/\partial K > 0$, i.e. a positive relationship between savings and capital stock. In particular, assumption (a) has been illustrated by Kaldor using an S-shaped investment function, or equivalently a savings function characterized by an inverted S-shape. The present Chapter is a dynamical exercise on the particular version of the Kaldor model introduced in Herrmann (1985), which has been studied also in Lorenz (1992, 1993), and in Dohtani *et al.* (1996). While in the aforementioned papers the focus was on chaotic dynamics, in our analysis we will explore different regimes of parameters, where the dynamical behavior is characterized by coexistence of attractors.

Our assumptions about consumption (C_t) and investment (I_t), which are the same as in Herrmann (1985), are stated and discussed below.

- **Consumption**

  At each time t, the consumption is a sigmoid shaped function of income:

$$C_t = c_0 + \frac{2}{\pi} c_1 \arctan\left(\frac{\pi c_2}{2c_1}\left(Y_t - Y^*\right)\right) \tag{2}$$

  where Y^* denotes the exogenously assumed equilibrium (or normal) level of income and c_0, c_1, c_2 are positive parameters. A qualitative plot of the consumption function (2) is given in Fig.1. The consumption is therefore an increasing function of income (ranging between $c_0 - c_1$ and $c_0 + c_1$):However, while for extreme values of income

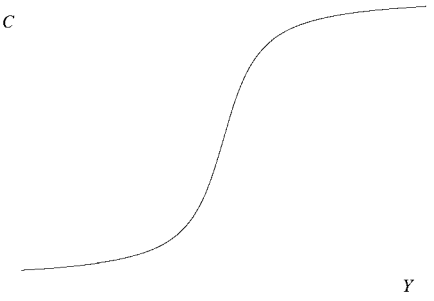

Figure 1: *Qualitative consumption function.*

consumption remains nearly constant, there exists a region around the normal level Y^* where consumption increases rapidly at a rate close to c_2, which represents the consumption propensity at Y^* (we assume $0 < c_2 < 1$).[1] The consumption function (2), or equivalently the inverted S-shaped savings function $S_t = Y_t - C_t$, reflects the view that the proportion of income which is saved is higher in non-ordinary periods, when Y_t is far from Y^*, because in such periods people perceive a larger portion of their income as being transitory[2].

- **Investment**

  At each time t, the investment is a linear function of income and capital stock. Precisely it is assumed that (gross) investment responds to a gradual adjustment of the actual capital stock to the desired capital stock, i.e.,

$$I_t = b\left(K_t^d - K_t\right) + \delta K_t$$

  where K_t^d is the desired stock of capital at time t, assumed linear in current output, that is $K_t^d = kY_t$, with k representing the desired *capital-output ratio* (which here will be considered as an exogenous parameter) and b, $0 < b < 1$, is the capital stock adjustment parameter. Therefore the investment function can be rewritten as a linear function of income and capital, as follows

$$I_t = bkY_t - (b - \delta)K_t \tag{3}$$

  where the Kaldorian negative relationship between investment and capital stock is fulfilled provided that $b > \delta$.

Substituting the consumption and investment functions (2)-(3) in model (1) we get

$$\begin{cases} Y_{t+1} = (1 - \alpha + \alpha bk)\, Y_t + (\alpha c_0 + \frac{2}{\pi} c_1 \arctan\left(\frac{\pi c_2}{2c_1}\left(Y_t - Y^*\right)\right) - \\ \qquad\qquad - (b - \delta)\, K_t) \\ K_{t+1} = b\left(kY_t - K_t\right) + K_t \end{cases} \tag{4}$$

[1] Given that Y^* is the turning point of the function (2), c_2 is the maximum propensity to consume.

[2] See Gallegati & Stiglitz (1993) for a model of business fluctuations where a similar consumption function is involved.

from which the coordinates of the exogenous steady state can be easily obtained

$$\begin{cases} Y^* = \frac{c_0}{1-k\delta} \\ K^* = kY^* = \frac{kc_0}{1-k\delta} \end{cases}$$

In order to simplify the analysis of the model (4), we normalize the steady state to $(0,0)$, by reformulating the model in terms of deviations

$$\begin{cases} x_t = K_t - kY^* \\ y_t = Y_t - Y^* \end{cases} \tag{5}$$

With the new coordinates (5), the dynamical system (4) is represented by the following map

$$T : \begin{cases} x' = (1-b)\,x + bky \\ y' = \alpha\,(\delta - b)\,x + (1 - \alpha + \alpha bk)\,y + \frac{2}{\pi}\alpha c_1 \arctan\left(\frac{\pi c_2}{2c_1}y\right) \end{cases} \tag{6}$$

where the symbol $'$ denotes the unit time advancement operator. Note first that the map T is independent on c_0, that is c_0 is only a "location" parameter and does not affect the asymptotic behavior of the system. Second, though the map T depends on 6 parameters, in our analysis we will assume b, k, δ, c_1 as fixed parameters, and we will perform stability and bifurcation analysis in the parameter space

$$\Omega = \{(\alpha, c_2) : \alpha > 0 \text{ and } 0 < c_2 < 1\}$$

8.3 General Properties of the Map

In this section we analyze some general properties of the map T in (6), which will play a role in the analysis of the global dynamics. Precisely we will discuss a symmetry property, the steady states and their local asymptotic stability, and the conditions of invertibility or noninvertibility of the map.

8.3.1 Symmetry Property

It can be easily checked that the map T is symmetric with respect to the origin $(0,0)$. This means that two points which are symmetric (with respect to the origin) are mapped into points which are also symmetric. This has important implications for attractors and basins of attraction of T. An immediate

consequence is that any invariant set of T either is symmetric with respect to the origin, or it admits a symmetric invariant set. In particular this holds for the fixed points and cycles of T. Thus, whenever further fixed points exist besides $(0,0)$, they must be in symmetric positions, and any cycle of T of odd period necessarily coexists with a symmetric one having the same characteristics. Moreover, the basins of attraction of the attracting sets of T either are symmetric or symmetric basins also exist.

8.3.2 Fixed Points and Local Stability Analysis

The equilibrium points of the model (6) are the fixed points of T, solutions of the system

$$\begin{cases} x = ky \\ \alpha(\delta - b)x + \alpha(bk - 1)y + \frac{2}{\pi}\alpha c_1 \arctan\left(\frac{\pi c_2}{2c_1}y\right) = 0 \end{cases}$$

Besides the trivial solution $E^* = (0,0)$, the map T may have further fixed points, whose y-coordinates satisfy

$$(1 - k\delta)y = \frac{2}{\pi}c_1 \arctan\left(\frac{\pi c_2}{2c_1}y\right)$$

Since the straight line of equation $z = (1 - k\delta)y$ and the sigmoid-shaped graph of the function $z = \frac{2}{\pi}c_1 \arctan\left(\frac{\pi c_2}{2c_1}y\right)$ intersect in three points if the slope of the straight line is positive and lower than that of the curve evaluated at the origin, we obtain the following

Proposition 1 *The map T in (6) has*

- *the unique fixed point $E^* = (0,0)$, if $(1 - k\delta) \leq 0$ or $c_2 \leq (1 - k\delta)$*
- *three fixed points, $E^* = (0,0)$ and two further points, P^* and Q^*, symmetric with respect to E^*, if $c_2 > (1 - k\delta) > 0$.*

The condition for the existence of further equilibria, stated in Proposition 1, has a straightforward interpretation, in that it can be rewritten as

$$(1 - c_2)Y^* < \delta k Y^* = \delta K^*$$

where the quantity $(1 - c_2)Y^*$ represents the savings at the exogenously assumed normal equilibrium, while δK^* is the amount of depreciation at the

same equilibrium. Therefore further equilibria exist if the equilibrium savings are insufficient to replace capital depreciation at the "normal" stationary state.

Let us now consider the local stability of the fixed point $E^* = (0,0)$. As usual, the analysis of local stability of a fixed point is obtained through the localization, in the complex plane, of the eigenvalues of the Jacobian matrix evaluated at the fixed point, and their dependence on the parameters of the model.

The Jacobian matrix of the map T in (6) is

$$J(x,y) = \begin{bmatrix} 1-b & bk \\ \alpha(\delta - b) & 1 + \alpha(bk-1) + \frac{\alpha c_2}{1+\left(\frac{\pi c_2}{2c_1}y\right)^2} \end{bmatrix} \tag{7}$$

and at E^* it specializes to

$$J^* = \begin{bmatrix} 1-b & bk \\ \alpha(\delta - b) & 1 + \alpha(bk - 1 + c_2) \end{bmatrix}$$

Observe that J^* does not depend on the parameter c_1: Then only five parameters are relevant in this context. To localize the eigenvalue of J^*, denoting by Tr its trace and by Det its determinant, we use the following well known necessary and sufficient condition [see e.g. Gumoswki & Mira (1980), Medio & Lines (2001)]:

i) $1 - Tr + Det = b\alpha(1 - c_2 - k\delta) > 0$

ii) $1 + Tr + Det = 2(2-b) - \alpha(2-b)(1-c_2) + \alpha bk(2-\delta) > 0$

iii) $1 - Det = b + \alpha(1-b)(1-c_2) - \alpha bk(1-\delta) > 0$

For fixed values of δ, k, b we can determine the region of local asymptotic stability of the steady state E^*, in the plane (α, c_2), as stated in the following

Proposition 2 *Assume* $\delta k < 1$, $b < 1$.

- *If* $b > \delta$ *and* $(2-b)^2 \geq bk(4 - 4\delta + \delta b)$ *the fixed point* $E^* = (0,0)$ *is locally asymptotically stable if the parameters* α *and* c_2 *belong to the region* $OABCD$ *of the plane* (α, c_2), *with vertices* $O = (0,0)$, $A = \left(\frac{2(2-b)}{2-b-bk(2-\delta)}, 0\right)$, $B = \left(\frac{(b-2)^2}{bk(b-\delta)}, \frac{(2-b)^2 - bk(\delta b - 4\delta + 4)}{(-2+b)^2}\right)$, $C =$

$\left(\frac{b}{k(b-\delta)}, 1-\delta k\right)$, $D=(0,1-\delta k)$, *where the sides AB, BC and CD belong to the hyperbola of equation*

$$c_2 = c_{2f}(\alpha) = \frac{\alpha-2}{\alpha} - \frac{bk(2-\delta)}{2-b} \tag{8}$$

to the hyperbola of equation

$$c_2 = c_{2N}(\alpha) = 1 + \frac{b-\alpha bk(1-\delta)}{\alpha(1-b)} \tag{9}$$

and to the line $c_2 = 1-\delta k$, *respectively;*

- *if* $b > \delta$ *and* $(2-b)^2 < bk(4-4\delta+\delta b)$ *the fixed point* $E^* = (0,0)$ *is locally asymptotically stable if the parameters* α *and* c_2 *belong to the region OBCD of the plane* (α, c_2), *with vertices* $O=(0,0)$, $B = \left(\frac{b}{bk(1-\delta)-(1-b)}, 0\right)$, $C = \left(\frac{b}{k(b-\delta)}, 1-\delta k\right)$, $D=(0,1-\delta k)$, *where the sides BC and CD belong to the hyperbola of equation*

$$c_2 = c_{2N}(\alpha) = 1 + \frac{b-\alpha bk(1-\delta)}{\alpha(1-b)}$$

and to the line $c_2 = 1-\delta k$, *respectively;*

- *if* $b < \delta$ *the fixed point* $E^* = (0,0)$ *is locally asymptotically stable if the parameters* α *and* c_2 *belong to the region OABD of the plane* (α, c_2), *with vertices* $O=(0,0)$, $A = \left(\frac{2(2-b)}{2-b-bk(2-\delta)}, 0\right)$, $B = \left(\frac{2-b}{k(\delta-b)}, 1-\delta k\right)$, $D=(0,1-\delta k)$, *where the sides AB and BD belong to the hyperbola of equation*

$$c_2 = c_{2f}(\alpha) = \frac{\alpha-2}{\alpha} - \frac{bk(2-\delta)}{2-b}$$

and to the line $c_2 = 1-\delta k$, *respectively.*
If $b = \delta$ *the vertex B is missing, because the hyperbola of equation* $c_2 = c_{2f}(\alpha)$ *approaches asymptotically the straight line of equation* $c_2 = 1-\delta k$ *for* $\alpha \to \infty$.

Moreover if the point (α, c_2) *exits the stability region by crossing the side AB, then a supercritical flip bifurcation occurs at which* E^* *becomes a saddle point and a period 2 attracting cycle appears; if the*

point (α, c_2) exits the stability region by crossing the side BC, then a Neimark bifurcation occurs at which E^* is transformed into an unstable focus; if the point (α, c_2) exits the stability region by crossing the side CD, then a supercritical pitchfork bifurcation occurs at which two stable fixed points are created close to E^*, which becomes a saddle.

Proposition 2 confirms analytically that the non-Kaldorian case $b \leq \delta$ (where the condition of inverse dependence of investment on capital stock is not fulfilled) cannot produce a Neimark bifurcation followed by self-sustained fluctuations of output and capital stock along a stable closed curve. On the other hand, in the opposite case $\delta < b$, self-sustained oscillatory behavior around the unstable steady state E^* occurs for sufficiently small values of c_2[3], i.e. when the propensity to save $1 - c_2$ is large enough, whereas for high values of c_2 the typical situation is that of two stable steady states P^* and Q^* and an unstable steady state E^*, located in the middle, i.e. a situation of *bi-stability* (without oscillations). For sufficiently small values of c_2, if condition $(2-b)^2 > bk(4 - 4\delta + \delta b)$ is fulfilled, also cycles of low period are possible, as a consequence of a flip bifurcation. This is what can be immediately deduced from the local analysis carried out in Proposition 2. However, global analysis will point out that long-run oscillatory behavior is possible even for high values of c_2 (beyond the pitchfork boundary), in parameter ranges where two further equilibria P^* and Q^* exist and are stable, or where they exist unstable but further stable periodic orbits exist. This will reveal phenomena of coexistence of the Kaldorian business cycle with other possible long-run dynamic outcomes, where the role played by the initial condition will be crucial.

8.3.3 Invertibility of the Map

Under particular parameters constellations, the map T in (6) is a noninvertible map of the plane. This means that while starting from an initial condition (x_0, y_0) the forward iteration of (6) uniquely defines the trajectory $(x_t, y_t) = T^t(x_0, y_0)$, $t = 1, 2, ...$, the backward iteration of (6) may not exist, or whenever it exists, may not be unique. Recent economic literature dealing with cases of multiple attractors in two-dimensional discrete-time dynamical systems represented by noninvertible maps [see e.g. Bischi & Kopel (2001), Dieci *et al.* (2001), Agliari *et al.* (2000)], has pointed out the

[3]Based on numerical evidence, we claim the supercritical nature of the Neimark bifurcation in this case.

role played by noninvertibility in bringing about bifurcations and complex structures of the basins of attraction. Complexity of the basins of attraction is also detected within the present model, though we must stress that in our case this is not due to the noninvertibility of the map. The goal of the present subsection is therefore to determine the regions of the space of parameters where the map is invertible (and noninvertible), in order to prove that the particular parameter constellation which will be adopted for our numerical simulation is one belonging to the invertibility region. Considering again the (α, c_2)-plane (for fixed values of the remaining parameters) so that the ranges of invertibility or noninvertibility of the map T can be compared with the local bifurcation curves, we can state the following proposition

Proposition 3 *The map T is invertible for any parameter combination (α, c_2) if $1 - b \leq bk(1 - \delta)$. In the opposite case $1 - b - bk(1 - \delta) > 0$, the non-invertibility region is an unbounded set defined by*

$$\begin{aligned} \alpha &> \tfrac{1-b}{1-b-bk(1-\delta)} \\ c_2 &> \tfrac{(\alpha-1)(1-b)-\alpha bk(1-\delta)}{(1-b)\alpha} \end{aligned} \tag{10}$$

Such a region has a vertex on the α-axis, given by $Z = \left(\frac{1-b}{1-b-bk(1-\delta)}, 0\right)$.

Proof. The rank-1 preimages of a point (u, v) are the solutions of the system

$$\begin{cases} u = (1-b)\,x + bky \\ v = \alpha\,(\delta - b)\,x + (1 - \alpha + \alpha bk)\,y + \frac{2}{\pi}\alpha c_1 \arctan\left(\frac{\pi c_2}{2c_1}y\right) \end{cases}$$

in the unknown variables x and y. Rearranging the two equations of such a system we obtain

$$\begin{cases} x = \frac{u-bky}{1-b} \\ v - \alpha\,(\delta - b)\,\frac{u}{1-b} + \frac{(\alpha-1)(1-b)-\alpha bk(1-\delta)}{1-b}y = \frac{2}{\pi}\alpha c_1 \arctan\left(\frac{\pi c_2}{2c_1}y\right) \end{cases}$$

Then the y-coordinates of the rank-1 preimages of the points (u, v) must satisfy the equation

$$q\,(u, v) + my = \frac{2}{\pi}\alpha c_1 \arctan\left(\frac{\pi c_2}{2c_1}y\right) \tag{11}$$

where $q(u,v) = v - \alpha(\delta - b)\frac{u}{1-b}$ and $m = \frac{(\alpha-1)(1-b)-\alpha bk(1-\delta)}{1-b}$.
It is simple to verify that if $m < 0$ or $m \geq \alpha c_2$, equation (11) has a unique solution for any given (u,v). Therefore if

$$\begin{cases} \frac{(\alpha-1)(1-b)-\alpha bk(1-\delta)}{1-b} < 0 \\ \frac{(\alpha-1)(1-b)-\alpha bk(1-\delta)}{1-b} \geq \alpha c_2 \end{cases}$$

holds, the map T is invertible, i.e. has a unique inverse. If $m = 0$, then a unique solution of (11) exists if $-\alpha c_1 < q(u,v) < \alpha c_1$, otherwise no solution exists.

In the case $0 < m < \alpha c_2$, one, two or three solutions of the equation (11) may exist depending on the value of $q = q(u,v)$. In particular, for a given m, two solutions exists if the straight line at the left side of (11) is tangent to the S-shaped curve $f(y) = \frac{2}{\pi}\alpha c_1 \arctan\left(\frac{\pi c_2}{2c_1}y\right)$, that is if

$$m = \frac{\alpha c_2}{1 + \left(\frac{\pi c_2}{2c_1}y\right)^2}$$

We obtain that the equation (11) admits two solutions if $q(u,v)$ becomes equal to q_1 or q_2, where

$$\begin{aligned} q_1 &= \frac{2c_1}{\pi c_2}\left[\sqrt{m(\alpha c_2 - m)} - \alpha c_2 \arctan\left(\frac{1}{m}\sqrt{m(\alpha c_2 - m)}\right)\right] \\ q_2 &= \frac{2c_1}{\pi c_2}\left[\alpha c_2 \arctan\left(\frac{1}{m}\sqrt{m(\alpha c_2 - m)}\right) - \sqrt{m(\alpha c_2 - m)}\right] \end{aligned}$$

Moreover, if $q(u,v) < q_1$ or $q(u,v) > q_2$ the equation (11) has a unique solution, while if $q_1 < q(u,v) < q_2$ three solutions exist.$\Diamond$

From Proposition 3 we deduce that, if

$$\begin{cases} \frac{(\alpha-1)(1-b)-\alpha bk(1-\delta)}{1-b} > 0 \\ \frac{(\alpha-1)(1-b)-\alpha bk(1-\delta)}{1-b} < \alpha c_2 \end{cases} \tag{12}$$

the map T is noninvertible and, following the notation used in Mira *et al.* (1996), it is a $Z_1 - Z_3 - Z_1$ map, which means that the phase plane is subdivided in different region Z_1 and Z_3, whose points have one and three different rank-1 preimages, respectively. Such regions, or *zones*, are separated by the *critical line LC*, i.e. the locus of points having two merging rank-1 preimages.

Thanks to the above computation, it is easy to obtain that the critical line is given by two distinct branches, that is $LC = L^a \cup L^b$ with

$$\begin{aligned} L^a &: y = \frac{\alpha(\delta - b)}{1 - b}x + q_1 \\ L^b &: y = \frac{\alpha(\delta - b)}{1 - b}x + q_2 \end{aligned} \tag{13}$$

The locus of the merging preimages of the points belonging to the set LC, is the rank-0 critical line LC_{-1} and it is given by $L^a_{-1} \cup L^b_{-1}$, where

$$\begin{aligned} L^a_{-1} &: y = -\frac{2c_1}{m\pi c_2}\sqrt{m(\alpha c_2 - m)} \\ L^b_{-1} &: y = \frac{2c_1}{m\pi c_2}\sqrt{m(\alpha c_2 - m)} \end{aligned}$$

i.e. the points which satisfy the tangency condition.

Such critical lines can be also obtained from the Jacobian matrix of the map T, indeed LC_{-1} is the locus of point at which the determinant of the Jacobian matrix (7) vanishes, and $LC = T(LC_{-1})$.

In particular, we are interested in the intersection of the noninvertibility region with the region of local stability of E^*. We restrict our analysis on the case $b > \delta$, which is the one of interest from the point of view of the dynamic analysis. Proposition 2 suggests that two different cases need to be considered.

- Case 1: $(2-b)^2 > bk(4 - 4\delta + \delta b)$. In such a case it is simple to show that the noninvertibility region (10) intersects the stability region of E^*, since the vertex B belongs to that region. In fact, the α- and c_2-coordinates of the vertex B satisfy the first and second inequality in (10), respectively.

- Case 2: $(2-b)^2 \leq bk(4 - 4\delta + \delta b)$. In such a case the map is invertible. In fact the condition $(2-b)^2 \leq bk(4 - 4\delta + \delta b)$ implies $1 - b - bk(1 - \delta) < 0$.[4]

[4]This result is derived by observing that in this case the intersection point between flip and Neimark bifurcation curves belongs to the half-plane $c_2 \leq 0$, and therefore the horizontal asymptote of the Hopf bifurcation curve must be negative, i.e. $1 - bk(1 - \delta)/(1 - b) < 0$. Given that $b < 1$, the latter condition implies $1 - b - bk(1 - \delta) < 0$.

In our analysis we shall consider constellations of parameters belonging to Case 2, under which the map T is invertible: The corresponding stability region of E^* is shown in Fig.2.

8.4 Global Dynamics Under Coexistence of Equilibria

As we have seen in Section 8.3, the local bifurcation curves of the "normal" steady state E^* suggest the existence of at least two different qualitative dynamic scenarios, outside the region of local asymptotic stability (see Fig.2). The first scenario, where α is small enough and c_2 is located just beyond its

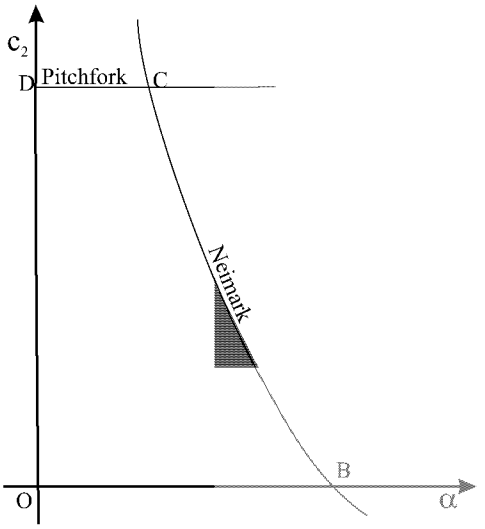

Figure 2: *Stability region of* E^*.

pitchfork bifurcation value $\widehat{c}_2 = 1 - \delta k$, is one where E^* is a saddle point and two further attracting steady states exist in the phase-space xy, on the line $y = x/k$, in symmetric positions with respect to E^* (bi-stability). The second scenario, where $c_2 < \widehat{c}_2$ and α is just larger than its Neimark bifurcation value, is one where the unique steady state $E^*$is an unstable focus and an attracting invariant closed curve exists around it in the phase space. As it is well known, however, the above results have only a local validity. In particular, nothing can be said in general about the survival of the attracting curve far from the Neimark bifurcation curve in the space of parameters: In

principle, it is possible that the attracting curve born via Neimark bifurcation is still surviving even for parameters far from the local stability region where in particular $c_2 > \widehat{c}_2$, i.e. where two further equilibria exist. This is precisely what happens in the case of the present model. Of course in similar cases [see also Agliari *et al.* (2005a,b)] a number of interesting questions are about the mechanisms which lead to the coexistence of an attracting closed curve with two further equilibria, the qualitative changes and the fate of the coexisting attractors (in particular the attracting curve) when the parameters are moved away from the region of stability, and the effects of changes of the parameters on the basins of attraction. These questions are the main topic of the present Section.

As we have also remarked in Section 8.3, other general properties of the map T in (6) may play a crucial role in the asymptotic behaviour of the system. One of this properties is the noninvertibility, which holds in the region (10) of the space of parameters: This may be in general at the origin of complex structures of the attractors and the basins of attraction (see the textbook Mira *et al.* (1996) and Chapter 1, Section 1.4). We rule out this possibility here, by choosing a regime of parameters under which the map T is invertible, in order to simplify as much as possible our understanding of the dynamic phenomena that we are going to analyze. Precisely, our analysis will be restricted to the region of invertibility of the map, and will follow a path in the parameter space through the region of existence of three fixed points, characterized by increasing values of α for a fixed value of $c_2 > \widehat{c}_2 = 1 - \delta k$. We will drive our attention to two different situations of coexistence of attractors, and to the associated bifurcations of attractors and basins: In the first one the two (locally) stable steady states born at the pitchfork bifurcation coexist with endogenous self-sustained oscillatory motion on an attracting closed curve; in the second one, where all the three steady states are unstable, the attracting curve coexists with periodic orbits of low period. A remarkable fact about the following examples is that they represent phenomena which occur when the selected parameters are far from the local bifurcation curves and therefore are due to global mechanisms. A second fact is that, though the two situations to be analyzed are apparently quite different from each other, they are ultimately determined by very similar mechanisms, associated with saddle connections and homoclinic tangles of some saddle cycle as described in Chapter 1 (to which we refer for technical details and symbolisms).

In the following we shall consider fixed values for the parameters k, b, δ, and c_1, given by $k = 1$, $b = 0.8$, $\delta = 0.25$, $c_1 = 2$. With these parameters, the pitchfork bifurcation occurs at $\widehat{c}_2 = 1 - \delta k = 0.75$. Therefore we

consider $c_2 > 0.75$, so that three fixed points exist, and increase α starting from $\widehat{\alpha} = \frac{16}{11} = 1.4545$, which is the α-coordinate of the vertex C in Fig.2.

8.4.1 Three Coexisting Attractors and Homoclinic Bifurcation of E*

Immediately after the pitchfork bifurcation of the exogenous steady state E^*, two attracting fixed points, the nodes P^* and Q^*, appear, located at symmetric positions with respect to the saddle E^*. Their basins of attraction are separated by the stable manifold $W^S(E^*)$. The unstable set $W^U(E^*)$ reaches the two fixed points: More precisely, a branch, say α_1, tends to P^* whereas the other one, say α_2, goes to Q^*.

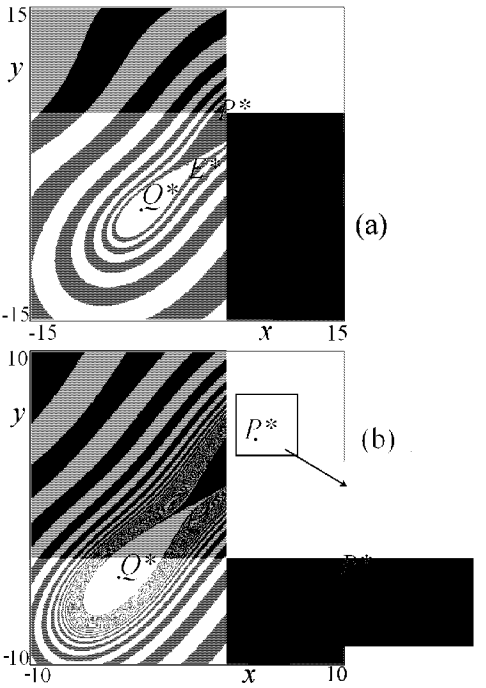

Figure 3: (a) $\alpha = 1.5; c_2 = 0.98$: *Basins of attraction of* P^* *and* Q^*. (b) $\alpha = 1.55; c_2 = 0.98$: *More and more convolutions of* $W^S(E^*)$ *appear.*

The phase portrait of Fig.3a shows an example of this situation: It has been obtained at $\alpha = 1.5$ and $c_2 = 0.98$, then quite far from the bifurcation.

Indeed at this parameter values the two nodes have turned into stable foci and the stable set of the saddle exhibits some convolutions separating the basins of attraction of P^* and Q^*, $\boldsymbol{B}(P^*)$ and $\boldsymbol{B}(Q^*)$ respectively (represented in Fig.3 with different gray tonalities).

As the speed of adjustment α increases, the set $W^S(E^*)$ involves more and more winging around the fixed points P^* and Q^*, as shown in Fig.3b. Consequently, the basin boundary appear to be more complicated and a trajectory starting from the region where the convolutions become thicker is subject to greater uncertainty about its long run behavior. In fact, a slight perturbation of an initial condition taken in such a region (see enlargement of Fig.3b) may cause a crossing of the basin boundary and consequently the convergence to a different equilibrium.

Moreover this basin structure suggests that some global bifurcation is about to occur. Indeed, when α is slightly increased, as in Fig.4a, an attracting closed curve Γ appears in the area where there was many convolutions of $W^S(E^*)$. This means that long-run quasi-periodic self-sustaining fluctuations are now a possible outcome, as well as dampened oscillations converging to the fixed points: Three typical trajectories, starting from initial condition taken in the three different basins, are represented versus time in Fig.4b.

The basins of attraction of P^* and Q^* are still separated by the stable manifold of the saddle E^*, but, differently from the case illustrated in Fig.3, now the preimages of the points of $W^S(E^*)$ accumulate on a repelling closed curve $\widetilde{\Gamma}$, appeared with Γ and very close to it (see enlargement in Fig.4a). The appearance of Γ and $\widetilde{\Gamma}$ could be due in principle to a "saddle-node" bifurcation for closed curves, given that the two curves are very close to each other, but we know that such a bifurcation is very quite rare in discrete maps. Then a mechanism similar to that described in Section 1.7 may be conjectured in this case: A saddle cycle appears via saddle-node bifurcation together with a repelling (or attracting) node cycle of the same period, then a saddle connection made up by the merging of two branches of the stable and unstable manifolds of the saddle gives rise to an attracting (or repelling) closed curve and to a heteroclinic connection between the periodic points of the two cycles made up by the stable (or unstable) set. These two invariant closed curves appear very close to each other and if the period of the cycle is very high they look like those of Fig.4a.

Whichever is the underlying mechanism, the appearance of the two invariant closed curves, one attracting and one repelling, has a noticeable effect on the asymptotic behaviour of the model, since three attractors now

coexist (the two equilibria, $P^*$and Q^*, and the closed curve Γ), the basins $\boldsymbol{B}(P^*)$ and $\boldsymbol{B}(Q^*)$ are strongly reduced and the majority of the trajectories are quasi-periodic (or periodic of very high period), since the curve $\widetilde{\Gamma}$ is now the basin boundary of Γ.

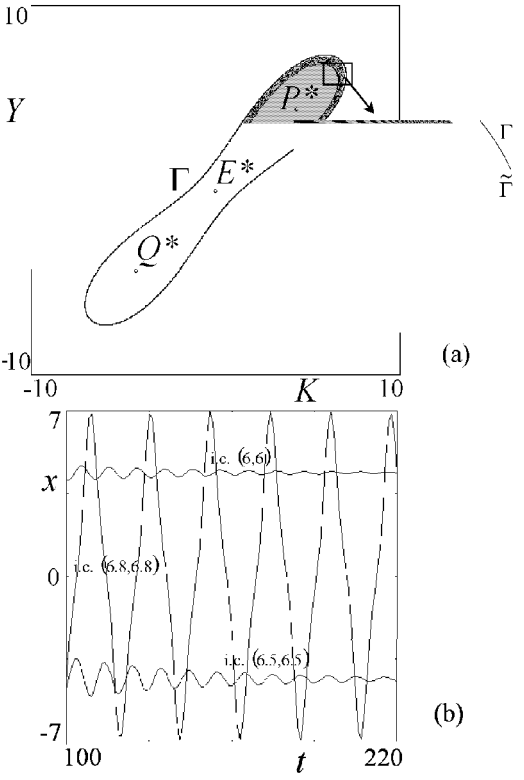

Figure 4: $\alpha = 1.552; c_2 = 0.98$: *Three coexisting attractors.* (a) *Phase space.* (b) *Three typical trajectories versus time.*

Moreover the repelling closed curve $\widetilde{\Gamma}$ is involved in other important qualitative changes in the structure of the basins of attraction as the adjustment speed is increased further. Indeed, as we can see in Fig.5a, it progressively reduces in size and shrinks in proximity of the saddle E^*. Up to now, initial conditions taken close to the exogenous equilibrium have produced trajectories converging to P^* or Q^*, but this is no longer true in the para-

meter constellation of Fig.5b, where trajectories starting close to E^* exhibit self-sustaining oscillations.

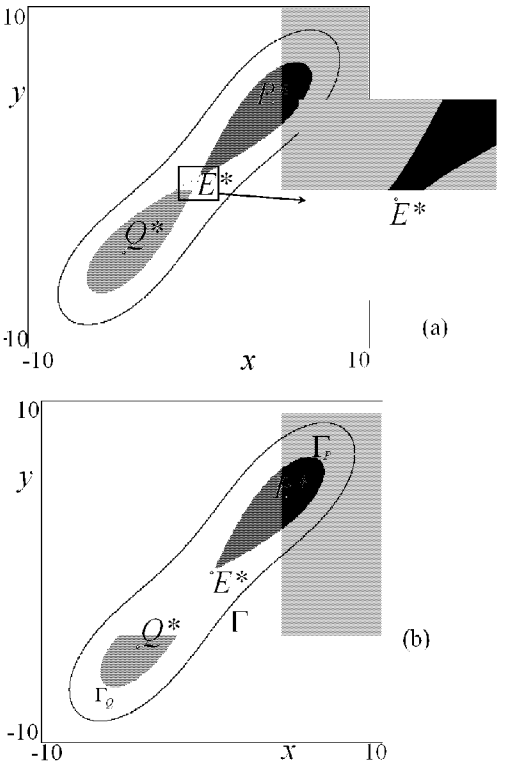

Figure 5: (a) $\alpha = 1.568; c_2 = 0.98$: *The repelling curve* $\widetilde{\Gamma}$ *shrinks in the proximity of* E^*. (b) $\alpha = 1.57; c_2 = 0.98$: $\widetilde{\Gamma}$ *is splitted into two repelling closed curves.*

This means that the points of the unstable manifold of E^* no longer reach the two equilibria but converge to Γ. This change in the asymptotic behaviour of $W^U(E^*)$ proves that a global bifurcation has occurred, involving both the unstable branches of the saddle E^*. Indeed in the phase portrait of Fig.5b we can observe the splitting of $\widetilde{\Gamma}$ into two repelling closed curves, Γ_P and Γ_Q, each one bounding the basin of the corresponding fixed point. These two repelling closed curves are the α-limit sets of the points of the two branches ω_1 and ω_2 of the stable set $W^S(E^*)$, which have modified

their behavior as well. Then we deduce that when the parameter α ranges from 1.568 to 1.57, a homoclinic bifurcation of E^* occurs, whose effect is the transition from one "large" repelling closed curve, basin boundary of the attracting set $\{P^*, Q^*\}$, to two "small" repelling closed curves, basin boundaries of $\boldsymbol{B}(P^*)$ and $\boldsymbol{B}(Q^*)$ respectively. This situation has been classified as *double homoclinic loop* in Chapter 1, since it involves both the branches of the stable and unstable sets of E^*: Its evolution, qualitatively described in Section 1.9 of that Chapter, is represented in Fig.6, where some enlargements of the phase space as well as of the stable and unstable sets of E^* are shown.

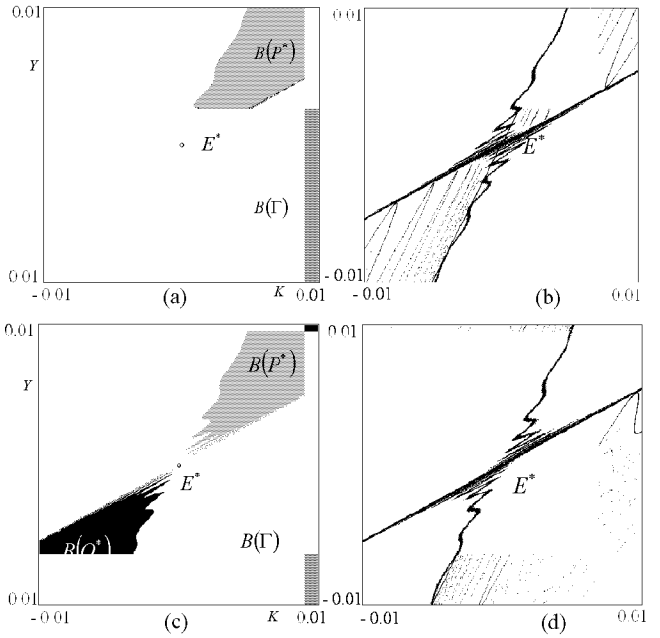

Figure 6: (a) $\alpha = 1.56855; c_2 = 0.98$: *Enlargement of the basins of attraction in the proximity of* E^*. (b) $\alpha = 1.56855; c_2 = 0.98$: *Stable (black) and unstable (gray) manifolds of* E^* *at the first tangency.* (c) $\alpha = 1.56855051; c_2 = 0.98$: *Enlargement of the basins of attraction in the proximity of* E^*. (d) $\alpha = 1.56855051; c_2 = 0.98$: *Stable (black) and unstable (gray) manifolds of* E^* *at the second tangency.*

The first homoclinic tangency is shown in Fig.6a,b, obtained at $\alpha = 1.56855$: The branch α_1 of $W^U(E^*)$ converges to P^* and it is completely contained in its basin of attraction; the same is true for α_2 with respect to the fixed point Q^*. The stable branches have a complex structure: The repelling closed curve Γ is replaced by a strange repellor, generated at the tangency and separating the basins of $\{P^*, Q^*\}$ and Γ. After the transversal crossing of $W^S(E^*)$ and $W^U(E^*)$, at which more and more homoclinic points of E^* are created, the second homoclinic tangency occurs at $\alpha = 1.5685501$, as shown in Fig.6c,d, and closes the tangle. The homoclinic points of E^* disappear as well as the chaotic repellor, leaving the two disjoint curves Γ_P and Γ_Q as boundaries of the basins of attraction of P^* and Q^*, respectively. After the homoclinic tangle both the branches of $W^U(E^*)$ converge to the attracting closed curve Γ and those of the stable set $W^S(E^*)$ come from the repelling closed curves Γ_P and Γ_Q.

A different illustration of this homoclinic tangle, occurring in a very narrow range of the parameter α, is proposed in Fig.7, where we show the as-

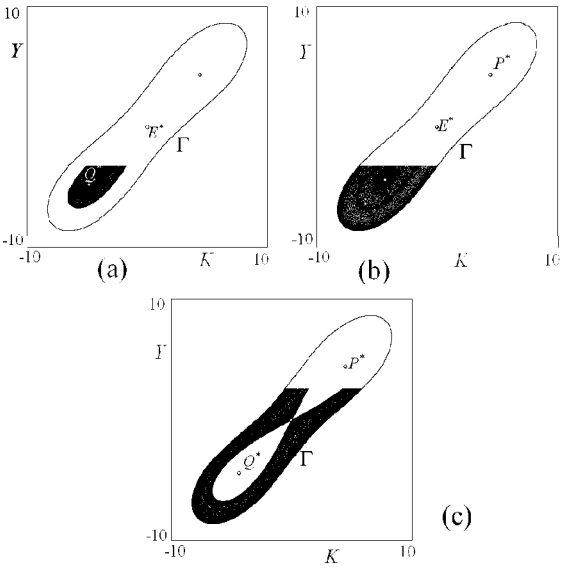

Figure 7: *The asymptotic behaviour of the unstable manifold of* E^* *at* (a) $\alpha = 1.56855; c_2 = 0.98$. (b) $\alpha = 1.5685503; c_2 = 0.98$. (c) $\alpha = 1.5685501; c_2 = 0.98$.

ymptotic behavior of the whole unstable set of the saddle E^*. In Fig.7a, obtained at the same parameter value as Fig.6a corresponding to the first homoclinic tangency, the points of $W^U(E^*)$ converge to the two equilibria, forming an eight-shaped structure; then, in fig.7b the unstable set $W^U(E^*)$ enters the basin of attraction of the attracting closed curve Γ as well as that of the attracting set $\{P^*, Q^*\}$: The separator of the three basins of attraction is a chaotic repellor, associated with the infinitely many periodic points existing close to the homoclinic trajectories. As α is further increased, more and more points of $W^U(E^*)$ converge to Γ until at the second homoclinic tangency, shown in Fig.7c, no points of the unstable set converge to the two stable foci.

As the parameter α further increases, the two repelling closed curves Γ_P and Γ_Q become smaller and smaller, until a new bifurcation value $\alpha = \widetilde{\alpha}_N$ is reached at which a Neimark subcritical bifurcation occurs: The two repelling closed curves collapse in P^* and Q^* respectively and at $\alpha > \widetilde{\alpha}_N$ the attracting closed curve Γ is the unique surviving attractor, since the two fixed points become unstable foci.

8.4.2 Coexistence of Cyclical and Quasi-Cyclical Trajectories and Homoclinic Loop of a Saddle Cycle

After the subcritical Neimark bifurcation of P^* and Q^*, the saddle E^* coexists with two repelling foci, from which the stable set $W^S(E^*)$ comes. The points of the unstable manifold $W^U(E^*)$ converges to the attracting closed curve Γ surrounding the three unstable fixed points.

This situation persists until at a certain value of α, say α_{sn}, a saddle-node bifurcation occurs, causing the appearance of two cycles of period 8, a saddle, S, and a stable node, C, which turns into a stable focus cycle immediately after. The two cycles are located outside the attracting closed curve and, as α increases from α_{sn}, a larger and larger portion of trajectories exhibits period-8 oscillations, as shown in Fig.8a, where the basins of attraction of the two attractors are represented in different gray tones. The points close to the exogenous equilibrium E^* still give rise to quasi-periodic fluctuations.

The phase portrait shown in Fig. 8b is completely different: Quasi-periodic and period-8 trajectories still coexist, but now the attracting closed curve $\widetilde{\Gamma}$ surrounds the stable focus cycle C and the majority of the trajectories exhibit quasi-periodic motion. Moreover the long run behaviour of trajectories starting in the area close to E^* is no longer predictable, since a small shock on them may have strong consequences given the many and many convolution of the separatrix of the two basins in this area.

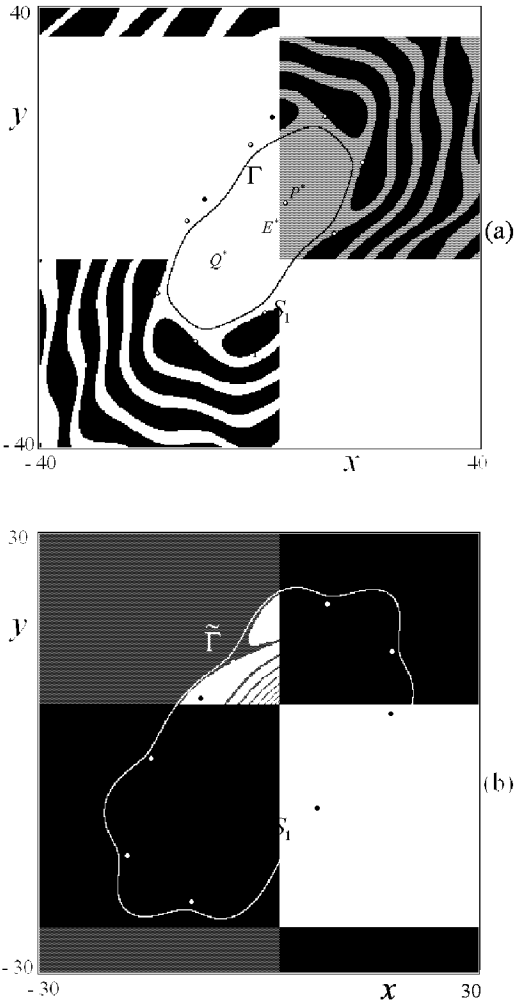

Figure 8: (a) $\alpha = 1.7; c_2 = 0.98$: *The attracting curve* Γ *coexists with a stable cycle* C *of period 8 and a saddle cycle* S *of the same period.* (b) $\alpha = 1.745; c_2 = 0.98$: *A new curve* $\widehat{\Gamma}$ *surrounds the attracting period 8 cycle.*

The aim of this subsection is to explain the global mechanisms which cause this important modification in the basin structures, transforming an attracting closed curve, coexisting with a stable cycle external to it, into a larger one, surrounding the stable cycle. As we shall see, the global bifurcation involved in this transition is of the same type of those described in Section 1.8, involving the invariant manifolds of the saddle cycle 8. Moreover, despite the different dynamic situation described here, the bifurcation mechanisms are similar to the ones analyzed in the previous section.

Let us start from Fig.8a, obtained at $\alpha = 1.7 > \alpha_{sn}$: Two attractors exist, the closed curve Γ and a focus cycle C, surrounding the curve, while the two basins, $\boldsymbol{B}(C)$ and $\boldsymbol{B}(\Gamma)$, are separated by the stable manifold $W^S(S) = \omega_1 \cup \omega_2$ of the saddle cycle S. The branches of the unstable one $W^U(S)$ reach the attracting closed curve (α_1) and the stable focus cycle (α_2). As the parameter α is increased, the two branches ω_1 and α_1 start to oscillate until a homoclinic tangency occurs. More precisely, at

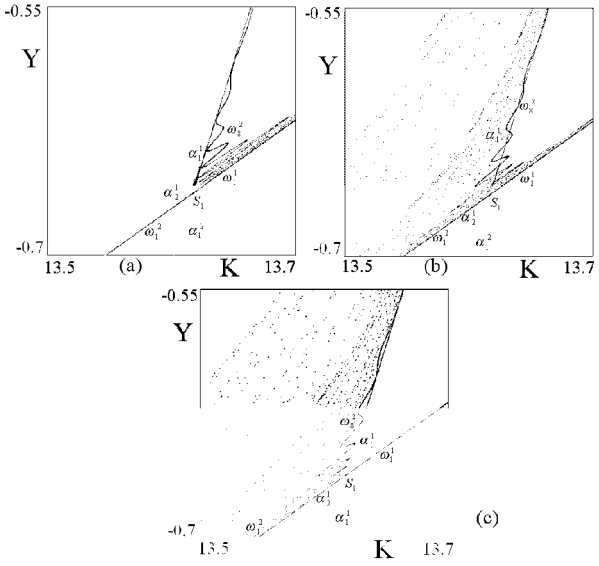

Figure 9: *Heteroclinic tangle involving the inner branches of stable and unstable manifolds of the cycle S.* (a) $\alpha = 1.7102384; c_2 = 0.98$: *First homoclinic tangency.* (b) $\alpha = 1.7102386; c_2 = 0.98$: *Transversal crossing.* (c) $\alpha = 1.7102387; c_2 = 0.98$: *Second homoclinic tangency.*

$\alpha = 1.7102384$ the stable branch $\alpha_{1,i}$ of the periodic point S_i has a tangential contact with the unstable branch $\omega_{1,j}$ of a different periodic point S_j (see Fig.9a) and this occurs cyclically for all the periodic points of the saddle S. This contact is the starting point of a heteroclinic tangle, which develops into a transversal crossing of the involved inner branches (Fig.9b) and closes at $\alpha = 1.7102387$, when a second cyclical homoclinic tangency occurs (Fig.9c). Observe that at the end of the heteroclinic tangle, the two branches α_1 and ω_1 have inverted they reciprocal position with respect to that of Fig.9a.

Approaching the heteroclinic tangle, the curve Γ exhibits more and more oscillations, as in Fig.10a obtained at the same parameter values of Fig.9a,

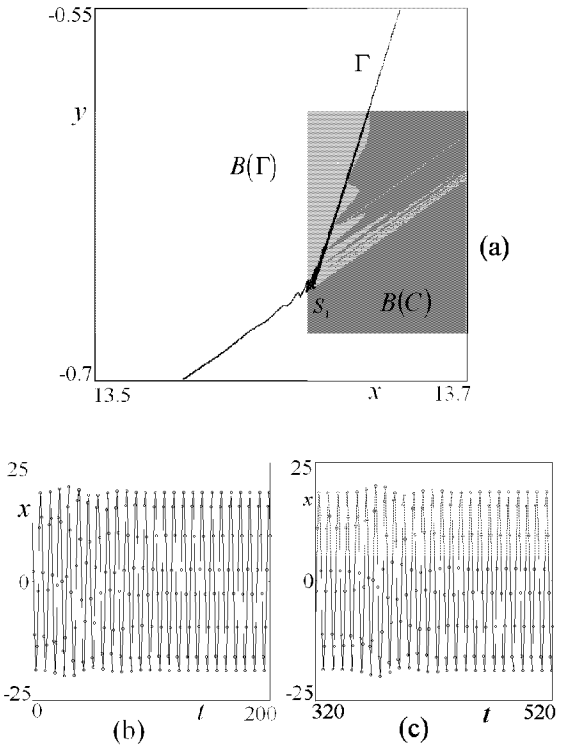

Figure 10: $\alpha = 1.7102384; c_2 = 0.98$. (a) *Oscillations of the attracting closed curve* Γ. (b-c) $\alpha = 1.7102386; c_2 = 0.98$: *Two different trajectories with initial conditions* (13.7,-0.7) *and* (13.5,-0.6) *respectively.*

before coming into resonance with the cycle, forming an attracting set with the saddle S and the focus cycle C, with C the attractor within it. Moreover during the tangle a chaotic repellor $\mathcal{R}$ is created in the area occupied by the transversal crossing of the two manifolds: The existence of $\mathcal{R}$ has important effects on the long run behaviour of the trajectories, as we can observe in Figs.10b,c, obtained at the same value of Fig.9b.

In such figures, two trajectories of the variable x are represented versus time and both converge to the cycle of period 8: In Fig.10b only a few iterations are needed to reach the period 8 oscillations whereas in Fig.10c a longer transient part exists (note that the first 320 iterations have been dropped in Fig.10c). This difference in the transient part is due to the initial conditions: The one of Fig.10c is taken in the area occupied by the chaotic repellor, and the existence of the infinitely many unstable cycle causes its particular behavior.

The effects of the observed heteroclinic tangle are illustrated in Fig.11: The attracting closed curve Γ has disappeared, leaving the focus cycle C as unique attractor (Fig.11b). More precisely, Γ has been replaced by the heteroclinic connection of the periodic points of the cycles, made up by the unstable manifold of the saddle S which reach the periodic points of the focus cycle (Fig.11a).With a similar mechanism the final situation of Fig.8b is obtained. Indeed, increasing α the two outer branches α_2 and ω_2 approach each other, oscillating. This is the prelude to a new heteroclinic tangle, again occurring in a very small range of the parameter α: The first tangential contact between the unstable branch $\alpha_{2,i}$ of the periodic point S_i and the stable branch $\omega_{2,j}$ of a different periodic point S_j is followed by their transversal crossing and then by the homoclinic tangency occurring at the opposite side with respect to the previous one (as illustrated in Fig.12a,b,c). A chaotic repellor appears at the first homoclinic tangency, persists during the transversal crossing phase and disappears at the closure of the tangle: Consequently, the trajectories starting close to it have a longer transient part before converging to the period 8 cycle. But the main effect of this global bifurcation is the appearance of an attracting closed curve $\widetilde{\Gamma}$, which replaces the heteroclinic connection between the periodic points of the cycles S and C. As soon as it has appeared, it exhibits many oscillations, as shown in Fig.13 obtained at the same parameter value as in Fig.12c, and surrounds the periodic points of the attracting cycle. As α increases, $\widetilde{\Gamma}$ becomes smoother and smoother reaching the shape of Fig.8b.

In order to discuss the results of our numerical analysis carried out in the last two sections, let us first remark that the original Kaldor's (1940) busi-

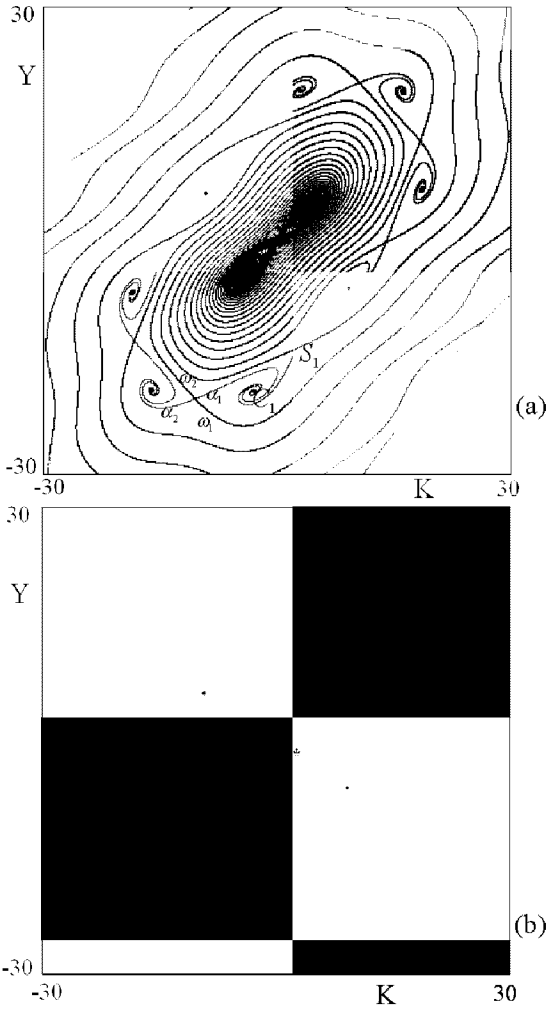

Figure 11: $\alpha = 1.72; c_2 = 0.98$: (a) *Heteroclinic connection made up by the unstable manifold of the saddle cycle S.* (b) *The period 8 focus cycle C is the unique attractor.*

ness cycle model - in spite of its simplicity and though it has been criticized on a number of grounds - is still present in modern treatments of business cycle theory and continues to stimulate pedagogical and methodological research (see e.g. Gabisch & Lorenz (1989)); such research is mainly oriented

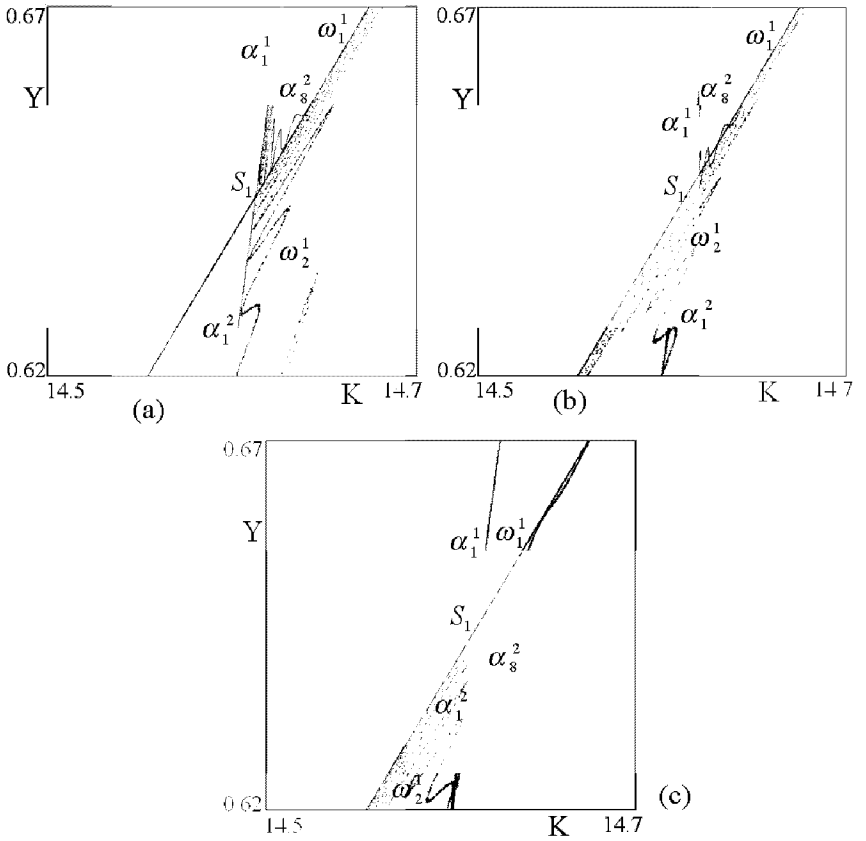

Figure 12: *Heteroclinic tangle involving the outer branches of stable and unstable manifolds of the cycle S.* (a) $\alpha = 1.74265991; c_2 = 0.98$: *First homoclinic tangency.* (b) $\alpha = 1.74266; c_2 = 0.98$: *Transversal crossing.* (c) $\alpha = 1.742660085; c_2 = 0.98$: *Second homoclinic tangency.*

to achieve a deeper understanding of the full range of dynamic outcomes compatible with the key qualitative assumptions of the model. Our contribu-

tion belongs to this stream of research, and focuses on particular phase-space transitions that determine two characteristic dynamic scenarios:

(i) the coexistence of two stable steady states and a stable closed curve, and the qualitative changes of their basins of attraction, in a regime of parameters where the exogenous, "normal" equilibrium is unstable (a saddle point);

(ii) the change of size and location of an attracting invariant curve with respect to a coexisting stable periodic orbit, in a parameter range where the map admits three unstable equilibria.

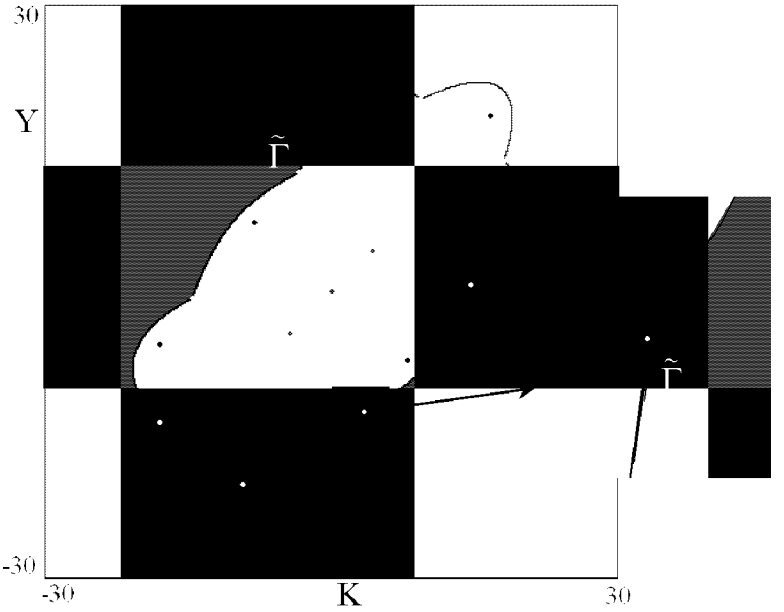

Figure 13: $\alpha = 1.742660085; c_2 = 0.98$: *The oscillations of the curve* $\tilde{\Gamma}$ *at its appearance.*

The main insight gained from our numerical and graphical investigation of such scenarios is that - though these phenomena look very different from each other at first sight - they are ultimately determined by the same kind of behavior of the stable and unstable set of the saddle point (in the first case), or of a saddle cycle (in the second case). Following the qualitative changes of stable and unstable manifolds closely, we have been able to detect numer-

ically particular ranges of the parameter where transversal intersections and homoclinic tangles exist, which proves the existence of chaotic behavior, and explains the complex structures of the basins of attraction in those particular situations. We remark once again that very similar dynamic phenomena have been detected also in a quite different version of the Kaldor model [Agliari *et al.* (2005b)], for plausible values of the parameters: This leads us to conjecture that such kinds of dynamic behavior might be ultimately related to the essential qualitative features of the original Kaldor model.

References

Agliari, A., 2001, "Global bifurcations in the basins of attraction in noninvertible maps and economic applications", *Nonlinear Analysis* 47, pp. 5241-5252.

Agliari, A., Bischi, G.I., Dieci, R., and Gardini, L., 2005a, "Global bifurcations of closed invariant curves in two-dimensional maps: A computer assisted study", *International Journal of Bifurcation and Chaos* 15, pp. 1285-1328.

Agliari, A., Bischi, G.I., and Gardini, L., 2002, "Some methods for the Global Analysis of Dynamic Games represented by Noninvertible Maps", Chapter 3 in *Oligopoly and Complex Dynamics: Tools & Models*, T. Puu and I. Sushko (eds.), Springer Verlag

Agliari, A., Dieci, R., and Gardini, L., 2005b, "Homoclinic tangles in a Kaldor-like business cycle model", *Journal of Economic Behavior & Organization*, to appear.

Agliari, A., Gardini, L., Delli Gatti, D., and Gallegati, M., 2000, "Global dynamics in a nonlinear model for the equity ratio", *Chaos, Solitons and Fractals* 11, pp. 961-985,

Bischi, G.I., Dieci, R., Rodano, G., and Saltari, E., 2001, "Multiple attractors and global bifurcations in a Kaldor-type business cycle model", *Journal of Evolutionary Economics* 11, pp. 527-554.

Bischi, G.I., and Kopel, M., 2001, "Equilibrium Selection in a Nonlinear Duopoly Game with Adaptive Expectations", *Journal of Economic Behavior and Organization* 46/1, pp. 73-100.

Dana, R.A., and Malgrange, P., 1984, "The dynamics of a discrete version of a growth cycle model", in *Analyzing the structure of economic models*, J.P. Ancot (Ed.), The Hague: Martinus Nijhoff, pp. 205-222.

Dieci R., Bischi, G.I., and Gardini, L., 2001, "Multistability and role of noninvertibility in a discrete-time business cycle model", *Central European Journal of Operation Research* 9, pp. 71-96.

Dohtani, A., Misawa, T., Inaba, T., Yokoo, M., and Owase, T., 1996, "Chaos, complex transients and noise: Illustration with a Kaldor model", *Chaos Solitons & Fractals* 7, pp. 2157-2174.

Gabisch, G., and Lorenz, H.W., 1989, *Business Cycle Theory*, 2nd edition, Springer-Verlag, New York.

Gallegati, M., and Stiglitz, J.E., 1993, "Stochastic and deterministic fluctuations in a nonlinear model with equity rationing", *Giornale degli Economisti e Annali di Economia* Anno LI (Nuova Serie) - Fasc. 1/4, pp. 97-108.

Grasman, J., and Wentzel, J.J., 1994, "Coexistence of a limit cycle and an equilibrium in a Kaldor's business cycle model and its consequences", *Journal of Economic Behavior and Organization* 24, pp. 369-377.

Gumowski, I., and Mira, C., 1980, *Dynamique Chaotique*, Cepadues Ed., Toulouse.

Herrmann, R., 1985, "Stability and chaos in a Kaldor-type model", DP22, Department of Economics, University of Gottingen.

Kaldor, N., 1940, "A model of the Trade Cycle", *Economic Journal* 50, pp.78-92, reprinted in *Essays on Economic Stability and Growth*, London, Duckworth, 1964, pp. 177-192.

Lorenz, H.W., 1992, "Multiple attractors, Complex Basin Boundaries, and Transient Motion in Deterministic Economic Systems", in *Dynamic Economic Models and Optimal Control*, G. Feichtinger (Ed.), North-Holland, Amsterdam, pp. 411-430

Lorenz, H.W., 1993, *Nonlinear Dynamical Economics and Chaotic Motion*, Second Edition, Springer-Verlag, New York.

Medio, A., and Lines, M., 2001, *Nonlinear Dynamics*, Cambridge University Press, Cambridge (UK).

Mira, C., Gardini, L., Barugola, A., and Cathala, J.C., 1996, *Chaotic Dynamics in Two-dimensional Noninvertible Map*, World Scientific, Singapore.